recommended as an initial treatment for MCHM when CV in tumour volume is above 1.8. Those patients should be treated by systemic chemotherapy and surgical resection then should be considered when the disease responds to the therapy.

Selecting the appropriate strategy according to the tumour staging has been an issue for patients with MCHM. Several studies proposed clinical risk scores incorporating the prognostic factors for predicting recurrence or prognosis after resection of MCHM to answer the clinical question.[4,8,11,23,24] However, those scoring systems and the factors consisting of each scoring system are not identical among the studies. The standard algorithm of treatment for MCHM is still obscure. Definitive and universal factors or a scoring system for predicting recurrence and prognosis after resection of MCHM is needed, and CV might be one of those factors in cases of MCHM.

The multistep process involving mutational events on both oncogenes and tumour suppressor genes is accepted for development of colorectal cancer, and several studies have shown that allelic imbalance correlated with staging and prognosis in colorectal cancer.[25,26] High CV might be caused by some genetic alterations. Genetic analysis such as evaluations of difference between the allelic imbalance of small tumours and that of large tumours in patients with high CV or evaluations of difference between the allelic imbalance of tumours in patients with low CV and that of tumours in patients with high CV may indicate particularly sensitive genomic regions and offer new information about the development of colorectal cancer. Further study is warranted to verify the prognostic significance of CV in tumour volume.

In conclusion, hepatic resections for MCHM sometimes contribute to long-term survival. Coefficient of variation in tumour volume above 1.8 might predict poor survival after hepatectomy of MCHM and be useful in planning the therapeutic strategy for patients with MCHM.

Acknowledgement

This work was supported in part by grants from Ministry of Health, Labor and Welfare, Japan.

References

1. Fortner JG, Silva JS, Golbey RB, Cox EB, Maclean BJ. Multivariate analysis of a personal series of 247 consecutive patients with liver metastases from colorectal cancer. I. Treatment by hepatic resection. *Ann Surg* 1984;**199**:306–16.
2. Steele Jr G, Bleday R, Mayer RJ, Lindblad A, Petrelli N, Weaver D. A prospective evaluation of hepatic resection for colorectal carcinoma metastases to the liver: Gastrointestinal Tumor Study Group Protocol 6584. *J Clin Oncol* 1991;**9**:1105–12.
3. Jamison RL, Donohue JH, Nagorney DM, Rosen CB, Harmsen WS, Ilstrup DM. Hepatic resection for metastatic colorectal cancer results in cure for some patients. *Arch Surg* 1997;**132**:505–10.
4. Fong Y, Fortner J, Sun RL, Brennan MF, Blumgart LH. Clinical score for predicting recurrence after hepatic resection for metastatic colorectal cancer: analysis of 1001 consecutive cases. *Ann Surg* 1999;**230**:309–18.
5. Choti MA, Sitzmann JV, Tiburi MF, Sumetchotimetha W, Rangsin R, Schulick RD, et al. Trends in long-term survival following liver resection for hepatic colorectal metastases. *Ann Surg* 2002;**235**:759–66.
6. Bolton JS, Fuhrman GM. Survival after resection of multiple bilobar hepatic metastases from colorectal carcinoma. *Ann Surg* 2000;**231**:743–51.
7. Scheele J, Stangl R, Altendorf-Hofmann A. Hepatic metastases from colorectal carcinoma: impact of surgical resection on the natural history. *Br J Surg* 1990;**77**:1241–6.
8. Nordlinger B, Guiguet M, Vaillant JC, et al. Surgical resection of colorectal carcinoma metastases to the liver. A prognostic scoring system to improve case selection, based on 1568 patients. Association Francaise de Chirurgie. *Cancer* 1996;**77**:1254–62.
9. Nakamura S, Suzuki S, Baba S. Resection of liver metastases of colorectal carcinoma. *World J Surg* 1997;**21**:741–7.
10. Cady B, Jenkins RL, Steele Jr GD, et al. Surgical margin in hepatic resection for colorectal metastasis: a critical and improvable determinant of outcome. *Ann Surg* 1998;**227**:566–71.
11. Iwatsuki S, Dvorchik I, Madariaga JR, et al. Hepatic resection for metastatic colorectal adenocarcinoma: a proposal of a prognostic scoring system. *J Am Coll Surg* 1999;**189**:291–9.
12. Bradley AL, Chapman WC, Wright JK, et al. Surgical experience with hepatic colorectal metastasis. *Am Surg* 1999;**65**:560–6.
13. Minagawa M, Makuuchi M, Torzilli G, et al. Extension of the frontiers of surgical indications in the treatment of liver metastases from colorectal cancer: long-term results. *Ann Surg* 2000;**231**:487–99.
14. Resection of the liver for colorectal carcinoma metastases: a multiinstitutional study of indications for resection. Registry of hepatic metastases. *Surgery* 1988;**103**:278–88.
15. Jass JR, Sobin LH. Histological typing of intestinal tumors. In: Jass JR, Sobin LH, editors. *World Health Organization. International histological classification of tumors*. 2nd ed. Berlin: Springer-Verlag; 1989.
16. Kaplan EL, Meier P. Non-parametric estimation from incomplete observations. *J Am Stat Assoc* 1958;**53**:457–81.
17. Cox DR. Regression models and life tables (with discussion). *J R Stat Soc B* 1972;**34**:187–220.
18. Couinaud C. Bases anatomiques des hepatectomies gaucle et droite reglees. *J Chirugie* 1954;**70**:933–66.
19. Weber SM, Jarnagin WR, DeMatteo RP, Blumgart LH, Fong Y. Survival after resection of multiple hepatic colorectal metastases. *Ann Surg Oncol* 2000;**7**:643–50.
20. Ostle B. *Statistics in research basic concepts and techniques for research workers*. 1st ed. Ames: Iowa State College Press; 1954.
21. Steel RGD, Torrie JH, Dickey DA. *Principles and procedures of statistics, a biometrical approach*. 3rd ed. New York: McGrawHill Book Co.; 1997.
22. Kato T, Yasui K, Hirai T, et al. Therapeutic results for hepatic metastasis of colorectal cancer with special reference to effectiveness of hepatectomy: analysis of prognostic factors for 763 cases recorded at 18 institutions. *Dis Colon Rectum* 2003;**46**:S22–31.
23. Nagashima I, Takada T, Matsuda K, et al. A new scoring system to classify patients with colorectal liver metastases: proposal of criteria to select candidates for hepatic resection. *J Hepatobiliary Pancreat Surg* 2004;**11**:79–83.
24. Ueno H, Mochizuki H, Hatsuse K, Hase K, Yamamoto T. Indicators for treatment strategies of colorectal liver metastases. *Ann Surg* 2000;**231**:59–66.
25. Weber JC, Schneider A, Rohr S, et al. Analysis of allelic imbalance in patients with colorectal cancer according to stage and presence of synchronous liver metastases. *Ann Surg* 2001;**234**:795–802. discussion 802–3.
26. Beau-Faller M, Weber JC, Schneider A, et al. Genetic heterogeneity in lung and colorectal carcinoma as revealed by microsatellite analysis in plasma or tumor tissue DNA. *Cancer* 2003;**97**:2308–17.

ANTICANCER RESEARCH *26*: 4705-4712 (2006)

Positron Emission Tomography with F-18 Fluorodeoxyglucose in Evaluating Colorectal Hepatic Metastasis Down-staged by Chemotherapy

SHINICHIRO TAKAHASHI[1], YOSHIHUMI KUROKI[2], KATSUHIRO NASU[2], SHIGERU NAWANO[2], MASARU KONISHI[1], TOSHIO NAKAGOHRI[1], NAOTO GOTOHDA[1], NORIO SAITO[3] and TAIRA KINOSHITA[1]

[1]*Department of Hepato-biliary Pancreatic Surgery,* [2]*Department of Diagnostic Radiology and* [3]*Department of Colorectal Surgery, National Cancer Center Hospital East, Chiba, Japan*

Abstract. *Background: The efficacy of positron emission tomography with ^{18}F fluoro-2-deoxy-D-glucose (FDG-PET) is obscure in evaluating viability or the extent of colorectal hepatic metastasis (CHM), down-staged by chemotherapy. Patients and Methods: A retrospective lesion-by-lesion analysis was performed for seven consecutive patients, who had received rescue hepatectomy for initially unresectable CHM, in order to evaluate the correlation between results of imaging modalities and the corresponding pathology. Results: The sensitivity and positive predictive value of the conventional modalities (CT and MRI) were 92% and 42%, respectively, while the sensitivity, specificity, positive predictive value and negative predictive value of FDG-PET were 58%, 100%, 100% and 75% respectively. The sensitivity of FDG-PET was 100% in evaluating the viability of tumors >2 cm, however, this fell to 17% in tumors <2 cm. Conclusion: FDG-PET is effective in assessing the viability of tumors >2 cm, but not those <2 cm, in patients with CHM down-staged by chemotherapy.*

Unresectable hepatic metastasis is one of the major obstacles in the treatment of colorectal cancer. Systemic chemotherapy for unresectable colorectal cancer has improved recently with the introduction of new effective agents (1-4). Even so, chemotherapy is rarely curative. Rescue hepatectomy after down-staging by chemotherapy is a potential treatment for unresectable colorectal hepatic metastasis (CHM) (5-8). However, pre-operative evaluation of tumor extent or viability is one of the issues in this strategy. The indication for rescue hepatectomy is based on the interpretation of the imaging of tumor extent or viability after down-staging by chemotherapy, however, evaluating the viability of hepatic tumors treated with chemotherapy is sometimes difficult by conventional imaging methods, such as computed tomography (CT) or magnetic resonance imaging (MRI), especially when the tumors have shrunk remarkably or exhibit notable calcification, after chemotherapy. Therefore, an effective diagnostic imaging modality to evaluate the viability of hepatic tumors after chemotherapy is needed.

Positron emission tomography with ^{18}F fluoro-2-deoxy-D-glucose (FDG-PET) is a functional imaging technique based on the increased utilization of glucose by tumor cells, and is effective for staging colorectal cancer (9, 10). Furthermore, the ability of FDG-PET to assess the pathological response to chemotherapy has been suggested in various malignant tumors (11-15). The correlation in CHM between FDG-PET findings and those of corresponding pathology has not been fully examined.

The present study was conducted to examine whether FDG-PET was able to assess tumor viability, before rescue surgery, for initially unresectable CHMs down-staged by chemotherapy and indicate which tumors should be resected.

Patients and Methods

Patient population. Seventy-four patients underwent hepatic resection for CHM at the National Cancer Center Hospital East, Japan, between January 2004 and July 2005, and 10 out of these underwent hepatic resection, after down-staging by chemotherapy. Since January 2004, all patients about to undergo rescue surgery are examined using FDG-PET pre-operatively, when informed consent is granted. Consequently, seven consecutive patients, who had been examined by CT, MRI and FDG-PET, were included in the present study. The patients were four men and three women, ranging from 44 to 70 years old. The location of the primary colorectal tumor was the colon in five patients and the rectum in two patients. All the

Correspondence to: Shinichiro Takahashi, MD, Department of Hepato-biliary Pancreatic Surgery, National Cancer Center Hospital East, 6-5-1 Kashiwanoha, Kashiwa 277-8577, Chiba, Japan. Tel: +81-471-33-1111, Fax: +81-471-31-4724, e-mail: shtakaha@east.ncc.go.jp

Key Words: Colorectal cancer, hepatic metastasis, chemotherapy, hepatic resection, FDG-PET.

0250-7005/2006 $2.00+.40

primary tumors were well- or moderately-differentiated adenocarcinomas. The primary tumors were staged as II (n=2), III (n=2), and IV (n=3) according to the TNM classification.

Chemotherapy. The reasons for choosing chemotherapy instead of curative resection, initially, were multiple bilobar tumors in five patients, invasion to the bilateral bile ducts and portal veins in one and invasion to the 3 major hepatic veins in one. The chemotherapies performed for the unresectable tumors were 5-fluorouracil-leucovorin combined with irinotecan in four patients, 5-fluorouracil-leucovorin alone in one, oral uracil/tegafur in one and capecitabine in one. Five patients experienced a partial response and two patients had stable disease, based on the Response Evaluation Criteria in Solid Tumors.

Conventional imaging (CT, MRI). All patients underwent contrast-enhanced CT and MRI before hepatectomy. Multi slice CT with 16 DAS was used for this study (Aquillion, Toshiba Medical Sysytems, Japan). CT images were obtained using 5 mm collimation after administration of 100 ml of nonionic iodine intravenous contrast medium injected at 3 ml/sec with a 70-sec delay (portal-dominant phase). Images were reconstructed at 5 mm intervals using a standard soft-tissue algorithm.

MR images were aquired using a 1.5-T MR imager (Gyroscan Intera, Philips Medical Systems, Netherlands) with a phased array coil. A section thickness of 7 mm with a 1 mm gap was used for all sequences. T1-weighted fast field-echo image, T2-weighted fast spin-echo image and diffusion-weighted image with b factor 500 sec/mm^2 were performed. After gadodiamide injection, T1-weighted fast field-echo dynamic image were also obtained during the hepatic arterial, portal venous and delayed phases.

FDG-PET. Whole body FDG-PET was performed in five patients using a GE Advance Scanner (General Electric Medical System, Milwaukee, WI, USA), which has an axial field of view of 15 cm and a spatial resolution of 4.5 mm full-width-half-maximum. All patients fasted for at least 4 h prior to scanning. Sixty min after intravenous injection of 300 MBq of F18-FDG, emission scanning was performed in 5 min and transmission scanning in 1 min. Data acquisition was performed in 7 bed positions.

In the remaining two patients, PET/CT scanning was performed using a Discovery LS PET/CT system (General Electric Medical Systems, Waukesha, WI, USA) because our PET system had been replaced by PET/CT. The CT component was performed using a multi-detector scanner. The parameters were 140 kV, 80 Ma, 0.8 s/CT rotation, a pitch of 6, and a table speed of 22.5 mm/s. Scans were acquired from the skull base to mid-thigh level, in 7 bed positions, with a total acquisition time of 31.9 sec to 37 sec. CT data was resized from a 512x512 matrix to a 128x128 matrix to match the PET data, to allow for image fusion and generation of CT transmission maps. The PET data were also acquired in the same anatomic positions: in 7 bed positions at 5 min per position.

All PET studies were performed at least 4 weeks after completion of chemotherapy.

Rescue hepatectomy. At the National Cancer Center Hospital East, Japan, all lesions considered positive for malignancy, by any pre-operative diagnostic imaging evaluation, were resected by rescue hepatectomy. During this operation, all the tiny suspicious lesions that were definitive metastases before chemotherapy were resected.

In our patients, a careful search was performed after laparotomy for local recurrence, extrahepatic metastases and peritoneal dissemination in the abdominal cavity. Any suspicious lesions were examined by biopsy. Intra-operative bimanual liver palpation and ultrasonography were performed to confirm tumor location and size, in all seven patients and all of the resections were ultrasound-guided procedures. Hepatic resection was performed with tumor-free resection margins, by the forceps fracture method, under inflow occlusion (Pringle's maneuver). When small lesions that had been detected by pre-operative imaging could not be recognized by either palpation or intra-operative ultrasonography, the estimated part or segment of the liver occupied by the lesions was resected.

Extended lobectomy and multiple partial resections were performed on two patients each, and central bi-segmentectomy, lobectomy, and segmentectomy were performed on one patient each, according to Couinaud's anatomical classification.

Assessment of tumor viability with FDG-PET. In our hospital, when interpreting conventional CT and MRI findings, any hepatic lesions are classified according to the degree of confidence that a metastatic tumor is present, as follows: definitely present, probably present, possibly present, probably absent and definitely absent. Lesions that fall into the definitely present, probably present and possibly present categories are considered positive for malignancy, while lesions that fall into the other categories are considered negative. Lesions which are positive, by either CT or MRI, are considered positive by conventional examination.

In the present study, the category "possibly present" included the small lesions, detected using conventional imaging, that were used to indicate definitive metastasis, but which then could not be determined as viable or otherwise, due to a reduction in size or remarkable calcification after chemotherapy (Figure 1).

All lesions considered positive by conventional examination were compared with their corresponding pathology findings, as the standard reference and the sensitivity and positive predictive value were then calculated. Furthermore, these lesions were also assessed by FDG-PET according to the degree of confidence of malignancy, *i.e.* definitely present, probably present, possibly present, probably absent, and definitely absent. A discrete focus with increased FDG accumulation, markedly greater than that in the hepatic parenchyma, was interpreted as malignancy, being definitely present or probably present. Focally increased FDG uptake, minimally greater than in the liver, was considered possibly positive for malignancy, but heterogeneous uptake in the hepatic parenchyma without a focal lesion was considered to indicate that malignancy was probably absent. Lesions in the definitely present, probably present and possibly present categories were considered positive for malignancy, while those in the probably absent and definitely absent categories were considered negative.

FDG-PET findings were also compared with the pathology findings, as the reference, and then sensitivity, specificity, positive predictive value and negative predictive value were calculated according to tumor size: <2 cm and >2 cm.

Finally, the sensitivities, specificities, positive predictive values and negative predictive values were compared between the subgroups according to tumor size. The results of each imaging test were interpreted by at least two experienced radiologists.

Pathological examination. The resected hepatic specimens were fixed in 10% phosphate-buffered formalin, sliced at 5 mm intervals and embedded in paraffin. The findings of all lesions, considered positive

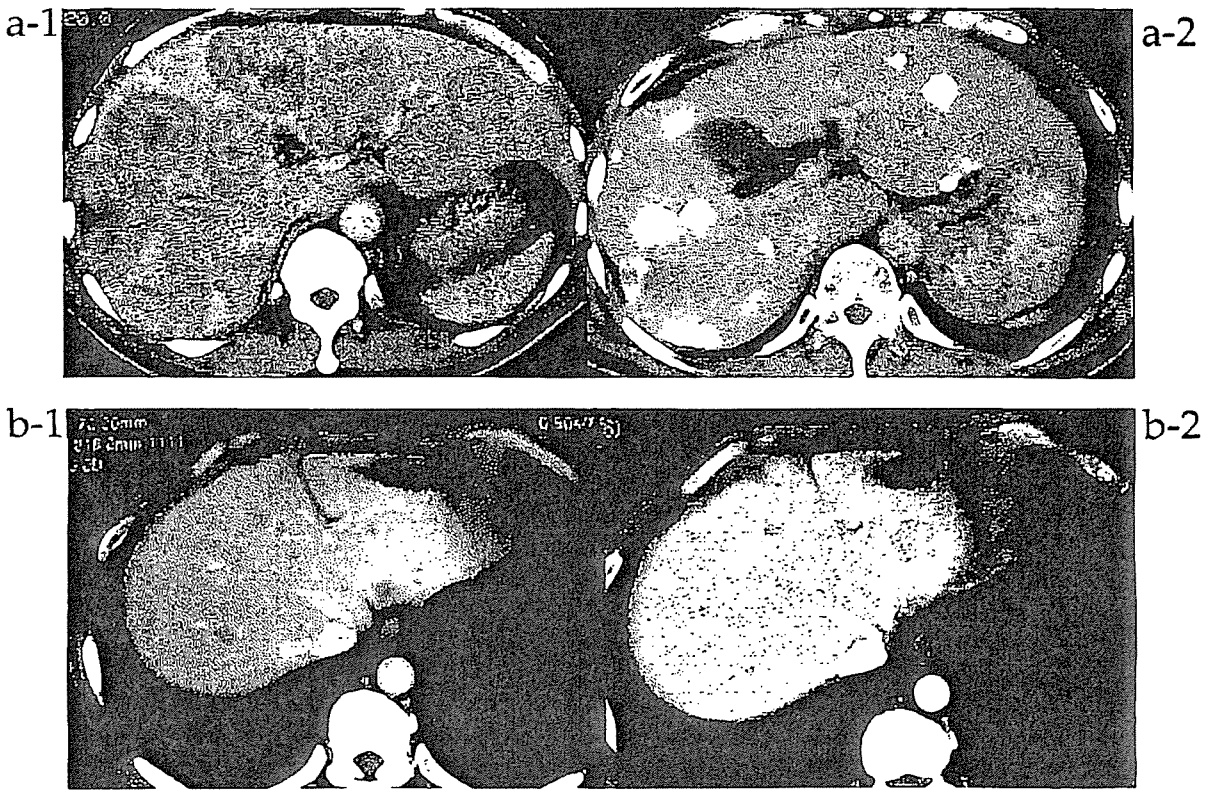

Figure 1. *a) A 45-year-old male with initially unresectable multiple colorectal hepatic metastases. (a-1) CT before chemotherapy. (a-2) CT after chemotherapy. Significant calcification was seen in the tumors. After rescue hepatectomy, histological examination revealed adenocarcinoma in most of the calcificated tumors. b) A 65-year-old female with multiple colorectal hepatic metastases. (b-1) CT before chemotherapy. (b-2) CT after chemotherapy. Tumors had reduced markedly in size.*

by any diagnostic imaging or intra-operative examination, were confirmed macroscopically and the lesions were then examined microscopically to evaluate viability. Serial sections 3 μm thick were stained with hematoxylin and eosin (H&E) for morphological examination. Histological diagnoses were based on the World Health Organization classification (16).

Statistical analysis. χ^2 analysis was used to assess sensitivity, specificity, positive predictive value and negative predictive value between subgroups according to tumor size. A *p*-value of less than 0.05 was considered to denote statistical significance.

Results

In the seven patients with CHMs down-staged by chemotherapy, 27 lesions were resected, all of which were considered positive for malignancy by pre-operative diagnostic imaging or intra-operative examination. Among the 27 lesions, 26 were deemed positive by at least one imaging modality, while the other could not be evaluated using imaging and was diagnosed by intra-operative examination. Twelve lesions were histologically diagnosed as adenocarcinoma, but no malignancies were demonstrated in the remaining 15 lesions.

Table I. *Comparisons of interpretations of CT, MR images and FDG-PET with pathology.*

	Pathological findings	
Imaging finding	Malignancy (12)	No malignancy (15)
CT and MR Imaging		
Positive (26)	11	15
Negative (1)	1	0
FDG-PET		
Positive (7)	7	0
Negative (20)	5	15

CT and MRI led to 26 lesions being diagnosed as malignant, while only 7 of these 26 lesions were considered positive by FDG-PET (Figure 2). No lesion was positive only by FDG-PET.

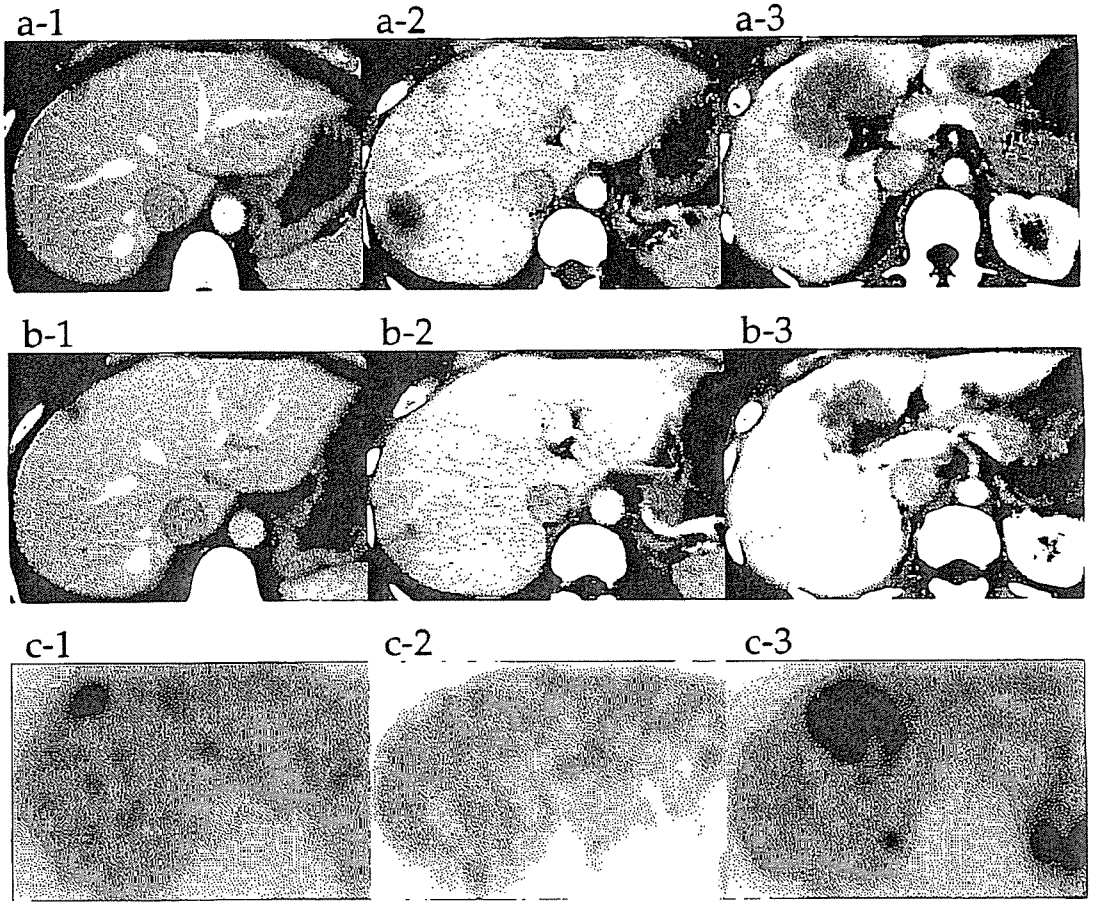

Figure 2. *A 44-year-old female with multiple colorectal hepatic metastases. (a-1, 2 and 3) CT before chemotherapy. Tumors were initially unresectable because of invasion to the hepatic hilum. (b-1, 2 and 3) CT after chemotherapy. Tumors in segments III, IV, V and VII showed significant reduction in size. (c-1, 2 and 3) FDG-PET after chemotherapy. By FDG-PET, tumors located in segments IV, V and VIII were considered positive, but tumors in segments III and VII were negative. Extended left lobectomy plus partial resections were performed. Tumors in segments III, IV, V and VIII proved histologically to be adenocarcinoma, but the tumor in segment VII had no viable cells.*

The interpretations of the conventional (CT/MRI) findings and FDG-PET findings were compared with the results of pathology in Table I. The sensitivity and positive predictive value of the conventional modalities were 92% (95% *CI*=0.73-1.00) and 42% (0.22-0.63), respectively, while the sensitivity, specificity, positive predictive value and negative predictive value of FDG-PET were 58% (95% *CI*=0.26-0.91), 100% (1.00-1.00), 100% (1.00-1.00) and 75% (0.54-0.96), respectively.

An assessment of the accuracy of conventional imaging and FDG-PET, according to tumor size (Table II), revealed that interpretation of the conventional findings and FDG-PET was highly accurate in lesions >2 cm. However, in lesions <2 cm, the positive predictive value for conventional imaging was only 26%, while the sensitivity for FDG-PET was only 17%, both of which were significantly lower than in lesions >2 cm. The specificity and negative predictive value of conventional imaging were not calculated, because lesions negative by both CT and MRI, were not resected, except for one which was diagnosed as positive by intra-operative examination. The viability of the 27 tumors could not be determined by any cut-off value of tumor-size (data not shown).

Discussion

We assessed the efficacy of FDG-PET in evaluating the tumor viability of CHM down-staged by chemotherapy, before rescue surgery. Our results indicate that FDG-PET is only effective in assessing the viability of hepatic lesions >2 cm after chemotherapy.

Table II. *Accuracies of CT, MRI, and FDG-PET in evaluation of tumor viability according to tumor size.*

	Sensitivity (%)	Specificity (%)	Positive predictive value (%)	Negative predictive value (%)	*P-value*
CT, MRI tumor size					
<2 cm	83 (5/6; 0.41, 1.00)	–	26 (5/19; 0.05, 0.48)*	–	<0.01*
≥2 cm	100 (6/6; 1.00, 1.00)	–	86 (6/7; 0.51, 1.00)*	–	
FDG-PET tumor size					
< 2 cm	17 (1/6; 0.00, 0.60)†	100 (14/14; 1.00, 1.00)	100 (1/1; –, –)	74 (14/19; 0.52, 0.96)	<0.01†
≥2 cm	100 (6/6; 1.00, 1.00)†	100 (1/1; 1.00, 1.00)	100 (6/6; 1.00, 1.00)	100 (1/1; –, –)	

Numbers in parentheses are the data used to determine the percentages and the 95% confidence intervals. *Difference between positive predictive value of CT and MRI in tumor <2 cm and that in tumor ≥2 cm. †Difference between sensitivity of FDG-PET in tumor <2 cm and that in tumor ≥2 cm.

The ability to use FDG-PET to assess the pathological tumor response to pre-operative chemotherapy, radiation or other treatment has been suggested in several tumors (11-15). In addition, correlation between decreased uptake in FDG-PET and histopathological response in the resected specimen was observed in patients, who underwent pre-operative chemotherapy or chemoradiotherapy for esophageal squamous cell carcinoma (17, 18), rectal cancer (19) and gastric carcinoma (20). However, the correlation between uptake in FDG-PET and the corresponding pathological findings has not been studied fully in CHM.

In the present study, portal phase helical CT and MRI were used as the conventional modalities. In our institution, diagnosis based on either, is routinely performed before hepatic resection for CHM, because portal phase helical CT has shown excellent sensitivity in detecting CHM and is considered as the standard pre-operative examination for CHM (21-23). Furthermore, SPIO-enhanced MRI and diffusion-weighted sensitivity encoding MRI have demonstrated high sensitivity equal to that of portal phase helical CT, and have excellent specificity in detecting CHM (24-26).

The present lesion-by-lesion analysis demonstrated that only 11 out of the 26 lesions that had pathological malignancy, considered positive for malignancy by conventional imaging. In the conventional examinations, the sensitivity of 92% for detecting hepatic viable CHMs was similar to that in the aforementioned studies, but the positive predictive value in tumors <2 cm was only 26%. Thus, CT and MRI were able to detect even small tumors, but could hardly evaluate the viability of small tumors after down-staging by chemotherapy.

On the other hand, FDG-PET showed excellent specificity (100%) and positive predictive value (100%), irrespective of tumor size. In tumors >2 cm, the sensitivity and negative predictive value for FDG-PET were both 100%. However, in tumors <2 cm, sensitivity was extremely low (17%). Thus, many of the tumors that shrunk to <2 cm by chemotherapy were undetectable by FDG-PET.

The reasons for this low sensitivity of FDG-PET in tumors <2 cm may be low spatial resolution, the partial volume effect and decreased FDG uptake in tumor tissue, after chemotherapy. Several groups reported that the sensitivity of FDG-PET for CHM was related to tumor size (27, 28). Lower sensitivity to smaller tumors was shown to be caused by the relatively low spatial resolution of FDG-PET and decreased measured activity concentration owing to the partial volume effect (29, 30). The partial volume effect reduces the measured activity concentration to a greater extent in smaller tumors.

Low sensitivity in FDG-PET has also been ascribed to the effects of chemotherapy itself. Chemotherapy may alter FDG uptake in two ways. First, the chemotherapy may reduce FDG uptake, by causing functional changes in tumor glucose metabolism. Spaepen *et al.* demonstrated that changes in tumor glucose metabolism occured rapidly after chemotherapy, as demonstrated using transplants of Daudi cells in SCID mice (31). Second, a decrease in viable cells by necrosis or apoptosis induced by chemotherapy may diminish FDG uptake in the tumor. Swisher *et al.* studied the correlation between the percentage of residual tumor and standardized uptake value (SUV) of FDG-PET after pre-operative chemoradiation in patients with esophageal cancer (18). They found that patients with >50% histological tumor viability had a significantly higher average SUV compared with those with <50% histological tumor viability. However, the SUV of tumors with no viability was similar to that of tumors with 10-50% tumor viability. Accordingly, when chemotherapy shows excellent efficacy in CHMs, it is extremely difficult to detect the resulting low FDG uptake by PET.

Our results suggest that the viability of small tumors that have been down-staged by chemotherapy can hardly be evaluated by CT, MRI or FDG-PET. Thus, at the moment, lesions considered positive by either CT or MRI should be treated by surgical resection in order to avoid leaving viable metastases in the residual liver. When surgical resection is not suitable for the specific lesion, perhaps due the small amount of residual liver, locoregional therapy, such as radiofrequency ablation or cryosurgery may become the preferred treatment options (6, 7).

The present study has nevertheless some limitations. The number of subjects in our study was relatively small, although the results have significant implications for rescue surgery for CHMs after chemotherapy. Furthermore, only two of the seven patients underwent PET/CT. The recent introduction of combined FDG-PET and CT has improved imaging accuracy by allowing accurate anatomical localization of FDG uptake. The sensitivity of PET/CT may be superior to that of FDG-PET for the detection of viable CHMs after chemotherapy. However, a major improvement in sensitivity is not expected, because the fundamental problem of detecting small viable tumors in PET is not resolved even using PET/CT.

New functional imaging with higher sensitivity for detecting small viable tumors is necessary to improve rescue surgery for CHM.

FDG-PET can be used to accurately assess the viability of CHMs >2 cm, before rescue surgery for initially unresectable CHMs down-staged by chemotherapy, but cannot be used for hepatic tumors <2 cm, because of the extremely low sensitivity of FDG-PET for such tumors.

Acknowledgements

This work was supported in part by grants from Ministry of Health, Labor and Welfare, Japan.

References

1 Goldberg RM, Sargent DJ, Morton RF, Fuchs CS, Ramanathan RK, Williamson SK, Findlay BP, Pitot HC and Alberts SR: A randomized controlled trial of fluorouracil plus leucovorin, irinotecan, and oxaliplatin combinations in patients with previously untreated metastatic colorectal cancer. J Clin Oncol *22*: 23-30, 2004.

2 Hurwitz H, Fehrenbacher L, Novotny W, Cartwright T, Hainsworth J, Heim W, Berlin J, Baron A, Griffing S, Holmgren E, Ferrara N, Fyfe G, Rogers B, Ross R and Kabbinavar F: Bevacizumab plus irinotecan, fluorouracil, and leucovorin for metastatic colorectal cancer. N Engl J Med *350*: 2335-2342, 2004.

3 Tournigand C, Andre T, Achille E, Lledo G, Flesh M, Mery-Mignard D, Quinaux E, Couteau C, Buyse M, Ganem G, Landi B, Colin P, Louvet C and de Gramont A: FOLFIRI followed by FOLFOX6 or the reverse sequence in advanced colorectal cancer: a randomized GERCOR study. J Clin Oncol *22*: 229-237, 2004.

4 Souglakos J, Androulakis N, Syrigos K, Polyzos A, Ziras N, Athanasiadis A, Kakolyris S, Tsousis S, Kouroussis Ch, Vamvakas L, Kalykaki A, Samonis G, Mavroudis D and Georgoulias V: FOLFOXIRI (folinic acid, 5-fluorouracil, oxaliplatin and irinotecan) vs. FOLFIRI (folinic acid, 5-fluorouracil and irinotecan) as first-line treatment in metastatic colorectal cancer (MCC): a multicentre randomised phase III trial from the Hellenic Oncology Research Group (HORG). Br J Cancer *94*: 798-805, 2006.

5 Fowler WC, Eisenberg BL and Hoffman JP: Hepatic resection following systemic chemotherapy for metastatic colorectal carcinoma. J Surg Oncol *51*: 122-125, 1992.

6 Rivoire M, De Cian F, Meeus P, Negrier S, Sebban H and Kaemmerlen P: Combination of neoadjuvant chemotherapy with cryotherapy and surgical resection for the treatment of unresectable liver metastases from colorectal carcinoma. Cancer *95*: 2283-2292, 2002.

7 Adam R, Delvart V, Pascal G, Valeanu A, Castaing D, Azoulay D, Giacchetti S, Paule B, Kunstlinger F, Ghemard O, Levi F and Bismuth H: Rescue surgery for unresectable colorectal liver metastases downstaged by chemotherapy: a model to predict long-term survival. Ann Surg *240*: 644-657, 2004.

8 Delaunoit T, Alberts SR, Sargent DJ, Green E, Goldberg RM, Krook J, Fuchs C, Ramanathan RK, Williamson SK, Morton RF and Findlay BP: Chemotherapy permits resection of metastatic colorectal cancer: experience from Intergroup N9741. Ann Oncol *16*: 425-429, 2005.

9 Ruers TJ, Langenhoff BS, Neeleman N, Jager GJ, Strijk S, Wobbes T, Corstens FH and Oyen WJ: Value of positron emission tomography with [F-18]fluorodeoxyglucose in patients with colorectal liver metastases: a prospective study. J Clin Oncol *20*: 388-395, 2002.

10 Fernandez FG, Drebin JA, Linehan DC, Dehdashti F, Siegel BA and Strasberg SM: Five-year survival after resection of hepatic metastases from colorectal cancer in patients screened by positron emission tomography with F-18 fluorodeoxyglucose (FDG-PET). Ann Surg *240*: 438-447, 2004.

11 Findlay M, Young H, Cunningham D, Iveson A, Cronin B, Hickish T, Pratt B, Husband J, Flower M and Ott R: Noninvasive monitoring of tumor metabolism using fluorodeoxyglucose and positron emission tomography in colorectal cancer liver metastases: correlation with tumor response to fluorouracil. J Clin Oncol *14*: 700-708, 1996.

12 Stroobants S, Goeminne J, Seegers M, Dimitrijevic S, Dupont P, Nuyts J, Martens M, van den Borne B, Cole P, Sciot R, Dumez H, Silberman S, Mortelmans L and van Oosterom A: 18FDG-Positron emission tomography for the early prediction of response in advanced soft tissue sarcoma treated with imatinib mesylate (Glivec). Eur J Cancer *39*: 7012-2020, 2003.

13 Juweid ME, Wiseman GA, Vose JM, Ritchie JM, Menda Y, Wooldridge JE, Mottaghy FM, Rohren EM, Blumstein NM, Stolpen A, Link BK, Reske SN, Graham MM and Cheson BD: Response assessment of aggressive non-Hodgkin's lymphoma by integrated International Workshop Criteria and fluorine-18-fluorodeoxyglucose positron emission tomography. J Clin Oncol *23*: 4652-4661, 2005.

14 Loi S, Ngan SY, Hicks RJ, Mukesh B, Mitchell P, Michael M, Zalcberg J, Leong T, Lim-Joon D, Mackay J and Rischin D: Oxaliplatin combined with infusional 5-fluorouracil and concomitant radiotherapy in inoperable and metastatic rectal cancer: a phase I trial. Br J Cancer *92*: 655-661, 2005.

15 Avril N, Sassen S, Schmalfeldt B, Naehrig J, Rutke S, Weber WA, Werner M, Graeff H, Schwaiger M and Kuhn W: Prediction of response to neoadjuvant chemotherapy by sequential F-18-fluorodeoxyglucose positron emission tomography in patients with advanced-stage ovarian cancer. J Clin Oncol *23*: 7445-7453, 2005.

16 Jass JR and Sobin LH: Histological typing of intestinal tumors. *In*: World Health Organization. International Histological Classification of Tumors, 2nd ed, Jass JR and Sobin LH (eds.). Berlin, Springer-Verlag, 1989.

17 Wieder HA, Brucher BL, Zimmermann F, Becker K, Lordick F, Beer A, Schwaiger M, Fink U, Siewert JR, Stein HJ and Weber WA: Time course of tumor metabolic activity during chemoradiotherapy of esophageal squamous cell carcinoma and response to treatment. J Clin Oncol *22*: 900-908, 2004.

18 Swisher SG, Erasmus J, Maish M, Correa AM, Macapinlac H, Ajani JA, Cox JD, Komaki RR, Hong D, Lee HK, Putnam JB Jr, Rice DC, Smythe WR, Thai L, Vaporciyan AA, Walsh GL, Wu TT and Roth JA: 2-Fluoro-2-deoxy-D-glucose positron emission tomography imaging is predictive of pathologic response and survival after preoperative chemoradiation in patients with esophageal carcinoma. Cancer *101*: 1776-1785, 2004.

19 Guillem JG, Moore HG, Akhurst T, Klimstra DS, Ruo L, Mazumdar M, Minsky BD, Saltz L, Wong WD and Larson S: Sequential preoperative fluorodeoxyglucose-positron emission tomography assessment of response to preoperative chemoradiation: a means for determining longterm outcomes of rectal cancer. J Am Coll Surg *199*: 1-7, 2004.

20 Ott K, Fink U, Becker K, Stahl A, Dittler HJ, Busch R, Stein H, Lordick F, Link T, Schwaiger M, Siewert JR and Weber WA: Prediction of response to preoperative chemotherapy in gastric carcinoma by metabolic imaging: results of a prospective trial. J Clin Oncol *21*: 4604-4610, 2003.

21 Kuszyk BS, Bluemke DA, Urban BA, Choti MA, Hruban RH, Sitzmann JV and Fishman EK: Portal-phase contrast-enhanced helical CT for the detection of malignant hepatic tumors: sensitivity based on comparison with intraoperative and pathologic findings. Am J Roentgenol *166*: 91-95, 1996.

22 Valls C, Andia E, Sanchez A, Guma A, Figueras J, Torras J and Serrano T: Hepatic metastases from colorectal cancer: preoperative detection and assessment of resectability with helical CT. Radiology *218*: 55-60, 2001.

23 Soyer P, Poccard M, Boudiaf M, Abitbol M, Hamzi L, Panis Y, Valleur P and Rymer R: Detection of hypovascular hepatic metastases at triple-phase helical CT: sensitivity of phases and comparison with surgical and histopathologic findings. Radiology *231*: 413-420, 2004.

24 Seneterre E, Taourel P, Bouvier Y, Pradel J, Van Beers B, Daures JP, Pringot J, Mathieu D and Bruel JM: Detection of hepatic metastases: ferumoxides-enhanced MR imaging versus unenhanced MR imaging and CT during arterial portography. Radiology *200*: 785-792, 1996.

25 Vogl TJ, Schwarz W, Blume S, Pietsch M, Shamsi K, Franz M, Lobeck H, Balzer T, del Tredici K, Neuhaus P, Felix R and Hammerstingl RM: Preoperative evaluation of malignant liver tumors: comparison of unenhanced and SPIO (Resovist)-enhanced MR imaging with biphasic CTAP and intraoperative US. Eur Radiol *13*: 262-272, 2003.

26 Nasu K, Kuroki Y, Nawano S, Kuroki S, Tsukamoto T, Yamamoto S, Motoori K and Ueda T: Hepatic metastases: diffusion-weighted sensitivity-encoding *versus* SPIO-enhanced MR imaging. Radiology *239*: 122-130, 2006.

27 Rohren EM, Paulson EK, Hagge R, Wong TZ, Killius J, Clavien PA and Nelson RC: The role of F-18 FDG positron emission tomography in preoperative assessment of the liver in patients being considered for curative resection of hepatic metastases from colorectal cancer. Clin Nucl Med *27*: 550-555, 2002.

28 Fong Y, Saldinger PF, Akhurst T, Macapinlac H, Yeung H, Finn RD, Cohen A, Kemeny N, Blumgart LH and Larson SM: Utility of 18F-FDG positron emission tomography scanning on selection of patients for resection of hepatic colorectal metastases. Am J Surg *178*: 282-287, 1999.

29 Geworski L, Knoop BO, de Cabrejas ML, Knapp WH and Munz DL: Recovery correction for quantitation in emission tomography: a feasibility study. Eur J Nucl Med *27*: 161-169, 2000.

30 Weber WA: Use of PET for monitoring cancer therapy and for predicting outcome. J Nucl Med *46*: 983-995, 2005.

31 Spaepen K, Stroobants S, Dupont P, Bormans G, Balzarini J, Verhoef G, Mortelmans L, Vandenberghe P and De Wolf-Peeters C: [(18)F]FDG PET monitoring of tumour response to chemotherapy: does [(18)F]FDG uptake correlate with the viable tumour cell fraction? Eur J Nucl Med Mol Imaging *30*: 682-688, 2003.

Received September 4, 2006
Accepted September 22, 2006

Surg Endosc (2006) 20: 1329–1331
DOI: 10.1007/s00464-005-0633-4

SURGICAL ENDOSCOPY
and Other Interventional Techniques

The application of a new stapling device for open surgery (Contour™ Curved Cutter Stapler) in the laparoscopic resection of rectal cancer

Y. Ishii, H. Hasegawa, H. Nishibori, T. Endo, M. Kitajima

Department of Surgery, School of Medicine, Keio University, Shinanomachi 35, Shinjuku-ku, Tokyo, 160-8582, Japan

Received: 13 September 2005/Accepted: 23 February 2006/Online publication: 8 June 2006

Abstract
Anastomotic leakage is a serious problem in the laparoscopic resection of rectal cancer. Although stapling devices and techniques for colorectal or coloanal anastomosis have been improved, laparoscopic anastomosis is still technically difficult and the rate of leakage is high. To resolve this problem, a new stapling device (the Contour™ Curved Cutter Stapler) for open surgery was applied to the laparoscopic resection of rectal cancer. After intracorporeal mobilization and vessel ligation, a 6-cm Pfannenstiel incision was made to insert the device into the peritoneal cavity, and a hand access device was placed on the site. The head of the device was put through a cutoff of the middle finger of a surgical glove, after which the wrist of the glove was attached to the hand access device. To prevent leakage of CO_2 gas through the gap between the shaft and the glove, the shaft covered by the glove was tied, and the gap was filled with bone wax. After re-creation of the pneumoperitoneum, the rectum was transected with the stapling device, and the anastomosis was accomplished by the double stapling technique. This technique enabled a reliable transection of the rectum because of the easy handling of the device and the wide laparoscopic view of the lower rectum in the deep pelvis.

Key words: Laparoscopic resection — Rectal cancer — Curved cutter stapler — Surgical glove — Double stapling technique

Laparoscopic surgery for rectal cancer has been reported to be feasible in selected patients [2, 4]; however, division of the rectum with laparoscopic linear staplers is sometimes treacherous, resulting in anastomotic leakage. In laparoscopic transection of the rectum, at least two linear staplers with a cutter are needed, and an unduly long staple line, often with an inadequate cutting angle is made, which is frequently associated with anastomotic leakage, although there are no data available concerning the number of staplers used and anastomotic leakage. A Pfannenstiel incision followed by the use of a conventional linear stapler for open surgery has been attempted [5], but this also is a challenging technique because of the poor visualization of the pelvis, and because the conventional stapler has no cutter. To obtain a reliable anastomosis, we have recently applied a new curved cutter stapler, designed for open surgery, in laparoscopic surgery for patients with rectal cancer.

Correspondence to: Y. Ishii

Technique

After high ligation of the inferior mesenteric vessels and pelvic dissection of the total mesorectum, a 6-cm Pfannenstiel incision to insert the curved head of the new stapling device (Contour Curved Cutter Stapler; Ethicon Endo-Surgery, Inc., Cincinnati, OH, USA) is made by extending the incision for the suprapubic trocar, and then a hand access device (LAP DISC; Ethicon Endo-Surgery, Inc.) is placed on the site. The middle finger of a surgical glove is cut, and the curved head of the Contour stapler is inserted into the glove through the cutoff of the middle finger. The gap between the shaft with the pin of the Contour and the glove is tied and filled with wax (Bone Wax; Ethicon Endo-Surgery, Inc.) to prevent leakage of CO_2 gas (Fig. 1). After the wrist of the glove is attached to the LAP DISC, pneumoperitoneum is re-established, and the curved head of the Contour stapler is inserted into the pelvic cavity with a wide laparoscopic field of view (Figs. 2 and 3). After rectal washout, transection of the rectum is performed, after which the anastomosis is created with a conventional circular stapler. We have encountered no problems with this technique for laparoscopic rectal resection since its introduction in our institute.

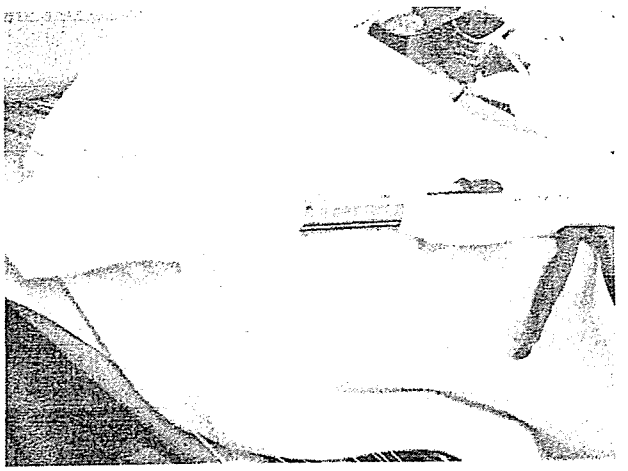

Fig. 1. Prevention of CO_2 gas leakage through the gap between the shaft of the Contour Curved Cutter Stapler and the glove.

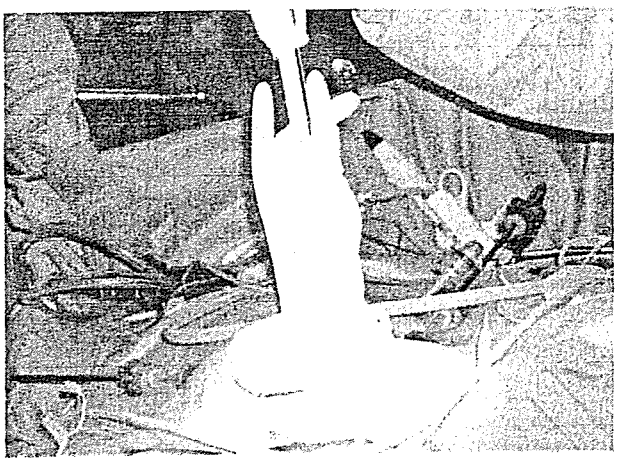

Fig. 2. Handling of the Contour stapler through the surgical glove under pneumoperitoneum.

Fig. 3. Laparoscopic view of the transection of rectum.

Discussion

Anastomotic leakage is a severe postoperative problem because of attendant life-threatening extensive peritonitis and an association with local recurrence [1]. Several risk factors related to anastomotic leakage following resection of rectal cancer have been reported, including male gender, pelvic drainage, a protective diverting stoma, a lower level of anastomosis, smoking, and excessive alcohol intake [3, 7–9]. Technical factors, which result from surgical complexity such as the mobilization of the rectum and the anastomosis in the narrow pelvis, also undoubtedly affect anastomotic complications [6].

In the double-stapling technique, the circular stapler used in laparoscopic surgery is basically the same as that used in open surgery. The authors used laparoscopic linear staplers through a suprapubic port to transect the rectum. Although articulated linear staplers are now available, at least two, and sometimes three or four staplers are needed, resulting in an unduly long staple line, which could be one of the reasons for anastomotic leakage. A Pfannenstiel incision followed by the use of a conventional linear stapler for open surgery has been attempted by some surgeons [4], but this also has limitations because it yields poor visualization of a deep, narrow pelvis, and the conventional stapler has no cutter.

Recently, the Contour stapling device, which has a small curved head and a cutter, has been used for rectal transection in open surgery. It is designed to reach even into a narrow pelvis and easily transect the rectum at one firing. The head of this device, with a 40-mm staple line is small, approximately 6 cm, which is similar in size to conventional staplers with a 30-mm staple line (TX/TL30; Ethicon Endo-Surgery, Inc. or TA30; United States Surgical, Tyco Healthcare Group LP, Norwalk, CT, USA). A 40-mm staple line is considered to be the ideal size to accommodate the rectum rather than a 30-mm line, and the incision to insert the Contour is also small, i.e., almost the same size as that required to remove the specimen from the abdomen in laparoscopic surgery.

In addition to the improvements to the head and cutter, the staple diameter of this device is smaller than a conventional stapler, yet the strength of stapled tissue is similar to that achieved with the conventional stapler. It enables a certain cutting of the transected rectum by the cutter of a circular stapler at anastomosis, and it can reduce the misfiring that results from an incomplete cutting by the stapler. Furthermore, with this device, the transected rectum is thoroughly stapled to the lateral edge, something that cannot be accomplished with conventional staplers, because the retaining pin is located within the staple line.

Because of the advantages presented by the Contour stapler compared with conventional staplers, the rate of anastomotic complications could be decreased. However, there have not yet been any reports about the usefulness or results of this device in either open or laparoscopic use.

We invented this technique to take advantage of both the usefulness of the Contour and the wide vision and space permitted by laparoscopy. Good visualization was achieved when pneumoperitoneum was maintained with the combined use of a Lap Disc, a surgical glove, and bone wax. The handling of the Contour is very smooth,

and this technique enables an easy approach to the deep pelvis, resulting in a reliable transection of the rectum.

There was no morbidity related to the anastomosis in our experience; however, further investigation is needed to evaluate this technique, and to compare the outcome with open procedures. Our technique enables the Contour stapler, originally designed for open surgery, to be used in laparoscopic surgery, but further improvement of this device is also anticipated, such as a columnar shaft to prevent leakage of CO_2 gas from the gap of the shaft.

Acknowledgments. The authors are indebted to Prof. J, Patrick Barron of the International Medical Communications Center of Tokyo Medical University for his review of this manuscript.

References

1. Branagan G, Finnis D, the Wessex Colorectal Cancer Audit Working Group (2005) Prognosis after anastomotic leakage in colorectal surgery. Dis Colon Rectum 48: 1021–1026
2. Guillou PJ, Quirke P, Thorpe H, Walker J, Jayne DG, Smith AM, Heath RM, Brown JM, the MRC CLASICC trial group (2005) Short-term endpoints of conventional versus laparoscopic-assisted surgery in patients with colorectal cancer (MRC CLASICC trial): multicentre, randomized controlled trial. Lancet 365: 1718–1726
3. Law WI, Chu KW, Ho JW, Chan CW (2000) Risk factors for anastomotic leakage after low anterior resection with total mesorectal excision. Am J Surg 179: 92–96
4. Leroy J, Jamali F, Forbes L, Smith M, Rubino F, Mutter D, Marescaux J (2004) Laparoscopic total mesorectal excision (TME) for rectal cancer surgery: long-term outcomes. Surg Endosc 18: 281–289
5. Lezoche E, Paganini AM, Feliciotti F (1997) A new technique to facilitate laparoscopic resection of low rectal tumors. Surg Laparosc Endosc 7: 9–12
6. Moran BJ (1996) Stapling instruments for intestinal anastomosis in colorectal surgery. Br J Surg 83: 902–909
7. Peeters KC, Tollenaar RA, Marijnen CA, Klein Kranenbarg E, Steup WH, Wiggers T, Rutten HJ, van de Velde CJ, the Dutch Colorectal Cancer Group (2005) Risk factors for anastomotic failure after total mesorectal excision of rectal cancer. Br J Surg 92: 211–216
8. Rullier E, Laurent C, Garrelon JL, Michel P, Saric J, Parneix M (1998) Risk factors for anastomotic leakage after resection of rectal cancer. Br J Surg 85: 355–358
9. Sorensen LT, Jorgensen T, Kirkeby LT, Skovdal J, Vennits B, Wille-Jorgensen P (1999) Smoking and alcohol abuse are major risk factors for anastomotic leakage in colorectal surgery. Br J Surg 86: 927–931

Annals of Surgical Oncology (© 2006)
DOI: 10.1245/s10434-006-9285-4

Effect of Combined Therapy With Low-Dose 5-Aza-2′-Deoxycytidine and Irinotecan on Colon Cancer Cell Line HCT-15

Megumi Ishiguro, MD, Satoru Iida, MD, PhD, Hiroyuki Uetake, MD, PhD, Shinji Morita, MD, Hiroshi Makino, MD, Keiji Kato, MD, Yoko Takagi, Masayuki Enomoto, MD, PhD, and Kenichi Sugihara, MD, PhD

Department of Surgical Oncology, Tokyo Medical and Dental University, Graduate School, 1-5-45, Yushima, Bunkyo-ku, Tokyo 113-8519, Japan

Background: Aberrant promoter hypermethylation is an epigenetic change that silences the expression of crucial genes, resulting in inactivation of the apoptotic pathway in various cancers. This hypermethylation can be restored by the demethylating agent 5-aza-2′-deoxycytidine (DAC). DAC might increase the tumor sensitivity to chemotherapy through demethylation and restoration of gene expression. We investigated the effect of combined therapy with DAC and irinotecan (CPT-11) on the human colon cancer cell line HCT-15.

Methods: Human colon cancer cell line HCT-15 was treated with DAC and/or CPT-11 both in vitro and in vivo. The changes in mRNA expression of several apoptosis-related genes were investigated by reverse transcriptase polymerase chain reaction (PCR). Promoter methylation was detected by methylation-specific PCR and combined bisulfite restriction analysis. Suppression of tumor growth was observed during the treatment with DAC and/or CPT-11 and apoptosis in the tumors was investigated by TUNEL (terminal deoxynucleotidyl transferase dUTP nick-end labeling) assay.

Results: Promoter methylation of $p14^{ARF}$, $p16^{INK4a}$, *BNIP3*, and *XAF1* was confirmed, and DAC restored mRNA expression of these genes. Demethylation and restoration of gene expression was observed with low-dose DAC, and demethylation status was sustained for several weeks. Combined therapy with DAC and CPT-11 produced marked suppression in tumor growth compared with DAC or CPT-11 alone, both in vitro and in vivo.

Conclusions: Pretreatment with low-dose DAC may have the potential to be used as a "biosensitizer" of DNA-damaging agents such as CPT-11 when the apoptotic pathway is inactivated as a result of aberrant promoter methylation in the cancer.

Key Words: Methylation—DAC—CPT-11—Chemosensitivity—Apoptosis.

Colorectal cancer (CRC) is one of the most common malignancies worldwide.[1] Chemotherapy is an important treatment strategy for metastatic CRC. One of the key chemotherapy drugs for treating metastatic CRC is irinotecan (CPT-11), a semisynthetic derivative of camptothecin and a potent DNA-topoisomerase I (topo-I) inhibitor that forms stable topo-I DNA-cleavable complexes and inhibits the progression of the replication fork.[2,3] CPT-11 has no cross-resistance with 5-fluorouracil (5-FU) and functions through a novel molecular mechanism.[4–6] The CPT-11–5-FU leucovorin combination is now approved as one of the standard chemotherapies for treating metastatic CRC.[4,7,8]

Several predictive factors of chemosensitivity have been investigated. The specific target enzyme or metabolic enzyme of the chemotherapeutic agent

Received August 25, 2006; accepted October 30, 2006
Address correspondence and reprint requests to: Megumi Ishiguro, MD; E-mail: ishiguro@tmde.ac.jp

could be one of the important predictive factors of chemosensitivity. Regarding 5-FU–based chemotherapy, the target enzyme TS (thymidilate synthase) and the metabolic enzyme DPD (dihydropyrimidine dehydrogenase) have been reported to be predictive factors,[9] whereas predictive factors of CPT-11 have not been sufficiently investigated.

In contrast, inactivation of the apoptotic pathway has been considered to be associated with chemoresistance.[10] Apoptosis induced by chemotherapy may be decreased as a result of dysfunction of apoptosis-related genes. Most chemotherapeutic agents such as CPT-11 and 5-FU damage DNA and induce apoptosis. When the apoptotic pathway is inactivated in the tumor, the tumor may become resistant to chemotherapy.

Aberrant hypermethylation of gene promoter CpG islands of cell-cycle regulator genes, apoptosis-related genes, and mismatch repair genes has been detected in various cancers.[11–13] Aberrant promoter hypermethylation in cancer cells can participate in inactivation of the apoptotic pathway at several points, either upstream (i.e., $p14^{ARF}$ or *DAPK*) or downstream (i.e., caspase) of the p53-dependent or p53-independent pathways.[1] This hypermethylation is the epigenetic change that silences the gene expression without altering nucleotide sequences. Such gene expression silenced as a result of hypermethylation can be restored by the demethylating agent 5-aza-2′-deoxycytidine (DAC).[14] DAC traps the DNA methyltransferase enzyme in a covalent complex with the DNA, resulting in a loss of DNA methylation with each cycle of cell division.[14,15] Many studies demonstrated that treatment with DAC restored the expression and the functions of a number of crucial tumor suppressor genes such as $p14^{ARF}$ and suppressed the growth of cancer cells in a heritable manner.[16–20]

Therefore, the clinical use of DAC in the treatment of cancers resistant to common anticancer drugs due to hypermethylation of tumor suppressor genes could potentially provide a novel approach to cancer treatment by restoring gene expression and increasing the sensitivity of cancer cells to common therapeutic regimens. However, the clinical efficacy of combined therapy with DAC and other chemotherapeutic agents has not been sufficiently investigated in solid tumors.

In the present study, we demonstrated the effect of combined therapy with DAC and CPT-11 on the human colon cancer cell line HCT-15, which has aberrant hypermethylation of several gene promoters. Plated cells and xenografts were treated with DAC followed by CPT-11. Then mRNA expression and methylation status of apoptosis-related genes were studied. We discuss the usefulness of DAC as a part of a combination chemotherapeutic approach.

MATERIALS AND METHODS

Reagents

CPT-11 and its active metabolite SN-38 were provided by Yakult (Tokyo, Japan). SN-38 was dissolved in dimethyl sulfoxide at a concentration of 1 μM and stored at −20°C, then further diluted in culture medium just before use. CPT-11 was dissolved in sterilized distilled water at a concentration of 5 mg/mL. After sonication at 70°C for 5 minutes, it was filter-sterilized and then stored at −20°C. DAC was obtained from Sigma (St. Louis, MO) and dissolved in phosphate-buffered saline (PBS) at a concentration of 10 μM for in vitro study and .1 mg/mL for in vivo study. It was filter-sterilized and stored at 4°C.

Cell Line

The human colon adenocarcinoma cell line HCT-15 was provided by Cell Resource Center for Biomedical Research, Tohoku University (Miyagi, Japan). The HCT-15 cell line is p53 deficient as a result of a point mutation and lacks $p14^{ARF}$ and $p16^{INK4a}$ expression because of promoter hypermethylation.[21,22] Cells were maintained in RPMI 1640 medium (Sigma) containing 10% heat-inactivated fetal bovine serum (FBS), 100 units/mL of penicillin, 100 μg/mL of streptomycin, 10 mM of HEPES (Gibco-BRL, Gaithersburg, MD), and 1.0 mM of sodium pyruvate (Gibco), and incubated at 37°C in 5% CO_2.

Effect of DAC on mRNA Expression and Methylation Status of HCT-15 In Vitro

Cells (1.25×10^4 per well) were plated in 24-well culture plates on day −2. On day 0, the culture medium was removed and new medium containing DAC was added. The cells were treated with 0, .1, .5, 1, or 5 μM of DAC for 72 hours, according to a previous report.[23] On day 3, the cells were rinsed twice with FBS-free medium and collected with trypsin-ethylenediaminetetraacetic acid (EDTA). RNA or DNA was extracted, and then the mRNA expression and methylation status of cell cycle related genes and

apoptosis-related genes were examined by reverse transcriptase (RT)-polymerase chain reaction (PCR) analysis.

To analyze the time course of mRNA expression after DAC treatment, .5 μM of DAC was added on day 0, and the medium was removed on day 3. The medium was exchanged every 3 days. Cells were collected every 3 days, and cDNA was prepared for real-time PCR analysis.

In Vitro Growth Inhibitory Activities of DAC

Cells ($.25 \times 10^4$ per well) were plated on day −2. Plated HCT-15 cells were treated with four protocols, as follows: group A, untreated control; group B, DAC alone; group C, SN-38 alone; and group D, DAC followed by SN-38. On day 0, the culture medium was removed and new medium containing .5 μM of DAC (or PBS) was added. On day 3, the cells were rinsed twice with FBS-free medium, and then new medium containing .005 μM of SN-38 (or PBS) was added. The dose of each drug was set on the bases of its pharmacological dose, results of previous reports,[23–25] and our preliminary experiments (data not shown). The cells were collected with trypsin-EDTA, stained with trypan blue, and counted daily. Each experiment was performed in triplicate. After the drug treatment, RNA was extracted on day 6 for RT-PCR analysis.

In Vivo Growth Inhibitory Activities of DAC and Changes of mRNA Expression

HCT-15 cells were cultured then resuspended in FBS-free medium. On day −10, approximately 10^7 cells in .2 mL of PBS were injected subcutaneously into the right flank of 6-week-old male BALB/c (nu/nu) mice. After 7 days, when the mean tumor diameter was 5 mm, mice were randomized into four groups (five mice per group) as follows: group A, untreated control; group B, DAC alone; group C, CPT-11 alone; and group D, DAC followed by CPT-11. The dose of each drug was set on the basis of the results of preliminary experiments (data not shown). The most effective and nontoxic regimen of DAC was reported as being three doses of DAC at intervals of 3 hours.[19]

On day −3, DAC (1 mg/kg) was administered intraperitoneally (i.p.) at 18:00, 21:00, and 24:00 (total dose, 3 mg/kg per mouse). On days 0, 4, and 8, CPT-11 (40 mg/kg) was administered i.p. at 18:00. Untreated control mice or mice receiving a single agent received injections of .2 mL of PBS on the days of therapy. The mice were weighed daily, and the tumor volume was determined by the following equation: tumor volume = $\alpha \times \alpha \times \beta/2$ mm^3, where α is the shortest and β is the largest diameter of the tumor. The relative tumor volume was determined as follows: relative tumor volume = tumor volume on day x / tumor volume on day 0.

For the analysis of mRNA expression, the mice of group B were killed on days −3, 0, 3, 6, 9, and 16. The tumors were extracted, and RNA was prepared and used for real-time PCR analysis.

The protocol for this animal experiment was approved by the Institutional Animal Care and Use Committee of Tokyo Medical and Dental University, and the experiment was carried out following the Guidelines for Animal Experimentation in Tokyo Medical and Dental University based on the Guide for the Care and Use of Laboratory Animals.

RT-PCR

From the treated cells and xenografts, total cellular RNA was extracted with the RNeasy Mini Kit (Qiagen, Valencia, CA) with DNase treatment, as we reported previously.[26] cDNA was synthesized with Superscript II (RNase H(−) reverse transcriptase; Invitrogen, Carlsbad, CA) with 10 ng of extracted RNA. Then PCR was performed as described previously.[26] We used the following PCR conditions: the initial denaturation step was at 94°C for 2 minutes, followed by 26 to 38 cycles of denaturation for 1 minute at 94°C, annealing for 1 minute at 55 to 63°C, and extension for 1 minute at 72°C. As an internal control for RT-PCR analysis, glyceraldehyde-3-phosphate dehydrogenase (GAPDH) transcripts were amplified from the same cDNA samples. Primer sequences are listed in Table 1. After amplification, PCR products were loaded onto 2% agarose gels, stained with ethidium bromide, electrophoresed, and visualized under ultraviolet illumination.

Real-Time PCR

We selected *p14^{ARF}* mRNA expression as a marker of the demethylation status because the gene promoter of *p14^{ARF}* is fully methylated in HCT-15 cells and the cells lack the gene expression. *p14^{ARF}* cDNA sequences were amplified by quantitative PCR by a fluorescence-based real-time detection method (ABI Prism 7300 Real Time PCR System, Taqman; Applied Biosystems, Foster City, CA) according to the manufacturer's protocol. Nucleotide sequences of primers and probe are listed in Table 1. As an

TABLE 1. *Candidate genes and primer sequences*

Gene		Nucleotide sequence (5′ – 3′) Forward primer	Reverse primer	Annealing temperature (°C)	Product size (bp)
RT-PCR					
GAPDH		CAA CAG CCT CAA GAT CAT CAG C	TCC TAG ACG GCA GGT CAG GTC	60	307
P14ARF		GAG TGA GGG TTT TCG TGG	GCC CAT CAT CAT GAC CTG	60	153
p16INK4a		CAA CGC ACC GAA TAG TTA CGG	GCG CAG TTG GGC TCC G	55	105
topo-I		TCC GGA ACC AGT ATC GAG AAG A	CCT CCT TTT CAT TGC CTG CTC	60	114
bax		ATC CAG GAT CGA GCA GGG CG	ACT CGC TCA GCT TCT TGG TG	55	94
bcl-2		CGA CTT CGC CGA GAT GTC CAG	ACT TGT GGC CCA GAT AGG CAC CCA G	63	385
bcl-XL/S		CAT GGC AGC AGT AAA GCA AG	GCA TTG TTC CCA TAG AGT TCC	56	351(L) 162 (S)
BNIP3		GGA TGC AGG AGG AGA GCC T	CGA GGT GGG CTG TCA CAG T	57	184
Bad		TTT AAG AAG GGA CTT CCT CGC C	GAG CTT CCC CTG CCC AAG TT	59	119
XAF1		ATG GAA GGA GAC TTC TCG GT	TTG CTG AGC TGC ATG TCC AG	57	290
MSP					
P14ARF	M	GTG TTA AAG GGC GGC GTA GC	AAA CCC CTC ACT CGC GAC GA	63	122
	U	TTT TTG GTG TTA AAG GGT GGT GTA GT	CAC AAA AAC CCT CAC TCA CAA CAA	63	132
p16INK4a	M	TTA TTA GAG GGT GGG GCG GAT CGC	GAC CCC GAA CCG CGA CCG TAA	63	150
	U	TTA TTA GAG GGT GGG GTG GAT TGT	CAA CCC CAA ACC ACA ACC ATA A	63	151
BNIP3	M	ATT CGT TTC GCG TAC GCG TC	GCG TCG CCC ATT AAC CGC GA	62	88
	U	ATT TGT TTT GTG TAT GTG TTG TA	ACA TAC CCC ATT AAC CAC AA	51	88
COBRA					
XAF1	1st	GAG AAT TTT GAA GAT TTT TT	AAT TCC TAC ACA CC	43	151
	2nd	TTG AAG TTG TGG GTT GGG TTA T	AAA AAT CTC CTT CCA TAT TCT AC	55	110
Real-time PCR					
P14ARF		CCC TCG TGC TGA TGA TGC TAC TGA	CCC ATC ATC ATG ACC TGG TCT T	60	77
	Probe	CGT CTA GGG CAG CAG CCG CTT CC			

RT-PCR, reverse-transcriptase polymerase chain reaction; MSP, methylation-specific PCR; COBRA, combined bisulfite restriction analysis; PCR, polymerase chain reaction.

internal standard, each individual sample was normalized to its β-actin content. Relative quantification of *p14ARF* mRNA expression was calculated by the ΔΔCt method[27] by SDSv1.2 with RQv1.0 software (Applied Biosystems). Each experiment was performed in duplicate.

Methylation-Specific PCR

The methylation status of gene promoters was analyzed by methylation-specific PCR.[28] The DNA methylation pattern in the CpG islands of the respective promoters was determined by chemical modification of unmethylated but not methylated cytosines to uracil and subsequent PCR that used specific primers for either methylated or modified unmethylated DNA. Genomic DNA was prepared,[29] and extracted DNA was subjected to bisulfite treatment as described previously[30] with a DNA modification kit (Chemicon International, Temecula, CA). The modified DNA was used as a template for methylation-specific PCR. Primer sequences are listed in Table 1. After amplification, PCR products were electrophoresed on 2% agarose gels.

Combined Bisulfite Restriction Analysis

Combined bisulfite restriction analysis is a semiquantitative method used to measure methylation at specific methylation-sensitive restriction sites.[31] Bisulfite-modified DNA was amplified by nested PCR with specific primers for *XAF1*. The primer sequences and PCR conditions are listed in Table 1. PCR products were then digested with a specific restriction enzyme, *Taq*I (Toyobo, Osaka, Japan), at 65°C for 2 hours, and then electrophoresed on 2% agarose gels. In the examined region within the *XAF1* promoter, *Taq*I cleaves only the methylated alleles.

TUNEL Assay

Drug-dependent apoptosis was evaluated with ApopTag Plus Peroxidase In Situ Apoptosis Detection Kit (Chemicon International) according to the manufacturer's protocol. For in vitro study, cells (.25 × 10^4 per well) were seeded in Biocoat Cellware Poly-D-Lysine 2-well culture slides (Becton Dickinson, Sparks, MD) on day −2 and treated with .5 μM of DAC (from days 0 to 3), followed by .005 μM of

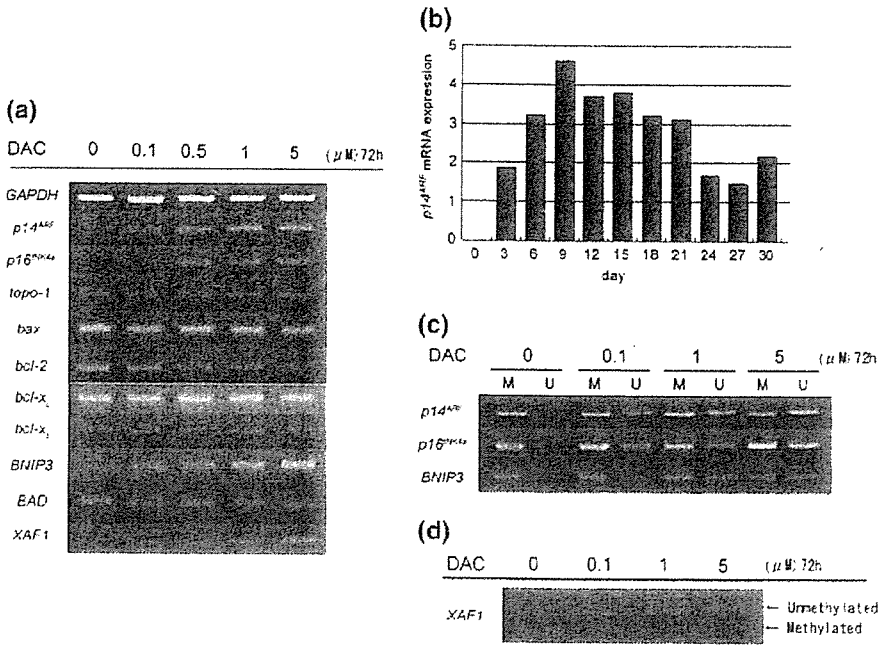

FIG. 1. (a) Changes in mRNA expression of apoptosis-related genes after demethylating agent 5-aza-2′-deoxycytidine (DAC) treatment. A total of 10 ng of RNA was extracted from the cells treated with 0, .1, .5, 1, and 5 μM of DAC for 72 hours and then used for reverse transcriptase polymerase chain reaction (RT-PCR). (b) Time course of $p14^{ARF}$ mRNA expression after DAC treatment. A total of .5 μM of DAC was added on day 0 and removed on day 3. RNA was extracted every 3 days. Relative quantification of $p14^{ARF}$ mRNA expression was investigated by real-time PCR. (c) Methylation-specific PCR analyzing the changes in the methylation status after DAC treatment. Lane M indicates existence of methylated DNA; lane U, existence of unmethylated DNA. (d) Combined bisulfite restriction analysis analyzing the changes in the methylation status of *XAF1* promoter after DAC treatment. Arrows indicate bands reflecting methylation of the *TaqI* sites.

SN-38 (from days 3 to 6). On day 6, the slides were washed with PBS and fixed for 15 minutes with 10% neutral buffered formalin, then used for TUNEL (terminal deoxynucleotidyl transferase dUTP nick-end labeling) assay. For in vivo study, treated mice were killed and the tumors were extracted on day 12. The tumors were fixed in 10% neutral buffered formalin. Tissues were embedded in paraffin, and 3-μm sections were cut. Paraffin was then removed from sections, and they were rehydrated and used for TUNEL assay. A dark brown staining indicated apoptosis. Ten representative areas without inflammation or necrosis were selected. TUNEL-positive cells from 10 fields per slide (×200 magnification) were counted under optical microscopy to calculate the mean ± SD.

Statistical Analysis

All statistical analyses were carried out with the StatView Software (version 5.0). Differences between the treatment groups were analyzed by Welch's *t*-test. Differences were considered statistically significant when $P < .05$.

RESULTS

Effect of DAC on mRNA Expression and Methylation Status in HCT-15

The changes in the mRNA expression of apoptosis-related genes in HCT-15 cells are shown in Fig. 1a. No mRNA expression of $p14^{ARF}$ and $p16^{INK4a}$ was identified in untreated HCT-15 cells. Expression of these genes was apparent with .1 μM of DAC. DAC clearly enhanced mRNA expression of $p14^{ARF}$, $p16^{INK4a}$, *BNIP3* (bcl-2 adenovirus E1B 19-kDa interacting protein 3), and *XAF1* (XIAP-associated factor 1) and decreased mRNA expression of *bcl-2* in a dose-dependent manner. However, the expression of bax and $bcl\text{-}X_{L/S}$ was unaffected by DAC. mRNA expression of *topo-I*, the target enzyme of CPT-11, was also unaffected by DAC.

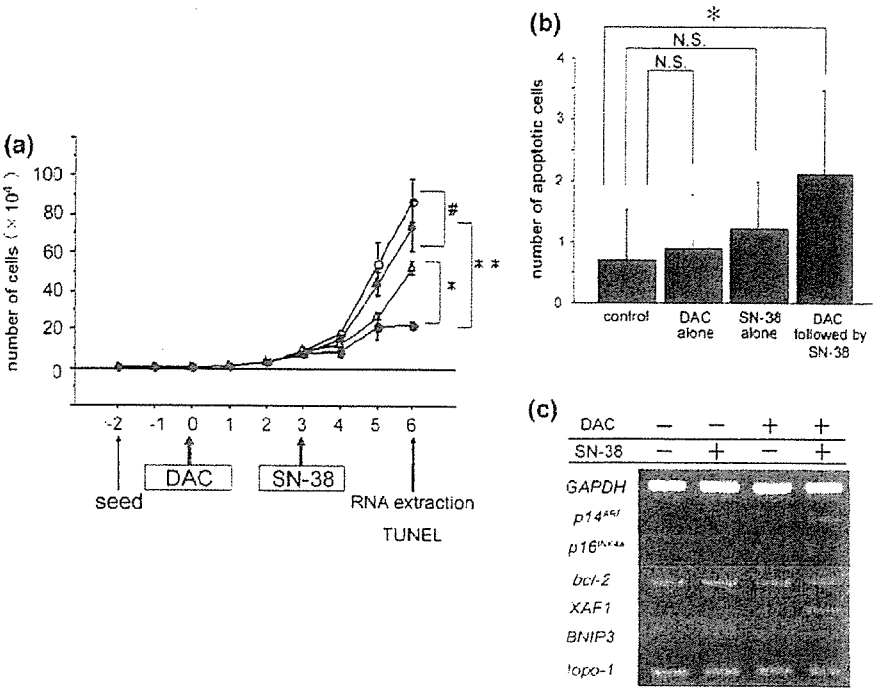

FIG. 2. (a) In vitro growth inhibition by demethylating agent 5-aza-2'-deoxycytidine (DAC) and/or SN-38. Plated HCT-15 cells were treated with four protocols, and numbers of cells were counted daily. DAC, .5 μM; SN-38, .005 μM. Open circle, group A (untreated control); solid triangle, group B (DAC alone); open triangle, group C (SN-38 alone); solid circle, group D (DAC followed by SN-38). * $P = .0009$, ** $P = .00216$, # $P = .0355$ (Welch's t-test). Error bars = SD. (b) Detection of apoptosis in vitro by TUNEL (terminal deoxynucleotidyl transferase dUTP nick-end labeling) assay. Data shown are mean number of TUNEL-positive cells counted in 10 fields per slide on day 6 in (a). * $P = .0126$ (Welch's t-test). Error bars = SD. (c) Changes in mRNA expression of apoptosis-related genes after DAC and/or SN-38 treatment. RNA was extracted on day 6 in (a), and then mRNA expression was investigated by reverse transcriptase–polymerase chain reaction.

The time course of $p14^{ARF}$ mRNA expression after DAC treatment is shown in Fig. 1b. In real-time PCR analysis, no mRNA expression of $p14^{ARF}$ was identified in untreated HCT-15 cells. $p14^{ARF}$ mRNA expression was apparent on day 3 and sustained for 30 days after .5 μM of DAC was removed on day 3.

By use of methylation-specific PCR and combined bisulfite restriction analysis, aberrant promoter methylation of $p14^{ARF}$, $p16^{INK4a}$, *BNIP3*, and *XAF1* was detected in untreated HCT-15 cells. After DAC treatment, the promoter demethylation of these genes was confirmed by the existence of unmethylated promoter regions (Fig. 1c,d).

Effect of DAC and/or SN-38 on Tumor Growth and Apoptosis In Vitro

The time course of the cell proliferation in vitro through the treatment of DAC and/or SN-38 is shown in Fig. 2a. On day 6, the number of cells in group D was 25% of that in group A, whereas those in groups B and C were 85% and 60%, respectively. The cell proliferation was suppressed in group D compared with groups A, B, and C. No marked suppression of the cell proliferation was observed in group B compared with group A. But there was a difference in cell proliferation between group A and C.

The mean number of apoptotic cells on day 6 determined by TUNEL assay is shown in Fig. 2b. The highest mean number of apoptotic cells was observed in group D, which was different from that in group A, whereas no difference was observed in the number of apoptotic cells between group B and group A as well as between group C and group A. Numerous mitotic cells were found in groups A, B, and C, but not in group D.

mRNA expression after the treatment with DAC and/or SN-38 on day 6 is shown in Fig. 2c. mRNA expression of $p14^{ARF}$, $p16^{INK4a}$, and *XAF1* was not identified in group C. The highest mRNA expression of these genes and the lowest mRNA expression of *bcl-2* were observed in group D. The expression of other apoptosis-related genes and *topo-I* gene was unaffected by combined therapy.

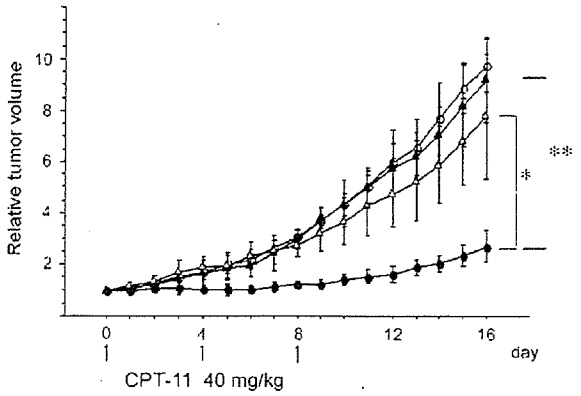

FIG. 3. In vivo growth inhibition by demethylating agent 5-aza-2'-deoxycytidine (DAC) and or CPT-11. Mice were treated with four protocols and the tumor volume was investigated daily. Data shown are mean relative tumor volume of five mice. DAC, 1 mg/kg intraperitoneally × 3; CPT-11, 40 mg/kg. Open circle, group A (untreated control); solid triangle, group B (DAC alone); open triangle, group C (CPT-11 alone); solid circle, group D (DAC followed by CPT-11). * $P = .0062$. ** $P = .0004$ (Welch's t-test). Error bars = SD.

Effect of DAC and/or CPT-11 on Tumor Growth and Apoptosis In Vivo

First, by use of real-time PCR, it was confirmed that DAC (1 mg/kg × 3) restored $p14^{ARF}$ mRNA expression in xenografts as in in vitro experiments. $p14^{ARF}$ mRNA expression was apparent after 3 days, maximal on day 6, and then sustained until the end of the experiment (Fig. 4a).

The relative tumor volumes in group D were far smaller compared with those of groups A, B, and C, and the growth rate remained lower on day 16, when the experiment ended (Fig. 3). The inhibition rate of tumor growth was highest in group D (Table 2). There was no difference in tumor growth among groups A, B, and C. At the dose used in this experiment, no body weight loss (Table 2) or lethal toxicity was observed. In the TUNEL assay, the mean number of apoptotic cells greatly increased in group D, like in the in vitro study (Fig. 4b).

DISCUSSION

In this study, DAC restored and increased the expression of apoptosis-related genes, including $p14^{ARF}$, *BNIP3*, and *YAF1*, in HCT-15 cells. Restoration of such genes through demethylation was observed even with low-dose DAC, and the demethylation status was sustained for several weeks after DAC was removed. Furthermore, combined treatment with DAC and CPT-11 markedly suppressed tumor growth compared with DAC or CPT-11 alone.

Normal cells express gene products that are related to the induction of apoptosis because of physiologically present biological response modifiers (BRMs). During carcinogenesis and tumor progression, expression of such gene products can be silenced by aberrant hypermethylation of promoter CpG islands. The reexpressed gene products that occur because of the demethylation of these genes by DAC might serve as a target for BRMs (administered in pharmacological doses), leading to subsequent cell death.[12] We hypothesized that apoptosis might be induced to a greater degree by the administration of anticancer drugs after demethylation of apoptosis-related genes by DAC treatment.

Paz et al.[11] studied 70 widely used human cancer cell lines of 12 different tumor types, including 11 CRC cell lines for CpG island promoter hypermethylation of 15 tumor suppressor genes, global 5-methylcytosine genomic content, and chemical response to the demethylating agent DAC, and found that CpG island of 11 CRC cell lines was hypermethylated in 25% to 60%. There was a great deal of 5-methylcitosine DNA content in the human cancer cell lines assessed, and the mean 5-methylcitosine DNA content was 3.3%. The highest level was found in the CRC cell line SW48 (5.6%). They also demonstrated that the 5-methylcitosine DNA content was greatly reduced in an average of 49% of cell lines after treatment with DAC. Petak et al.[32] reported that Fas promoter containing 28 CpG sites was methylated in the CRC cell lines Caco2 and RKO. And they demonstrated that DAC (1 μM, 72 hours) upregulated Fas expression and increased the percentage of apoptotic cells, furthermore sensitized RKO cells to recombinant FasL-induced apoptosis. They concluded that DNA hypermethylation may be one mechanism implying loss of sensitivity to Fas-induced apoptosis in CRC cells. These studies have demonstrated that cancer cells frequently contain promoter CpG island hypermethylation of tumor suppressor genes and DAC was expected to sensitize cancer cells to anticancer drugs.

$p14^{ARF}$, which is frequently inactivated in a variety of human cancers, is known to participate in the activation of the apoptotic pathway upstream of the p53-dependent pathway. In contrast, recent reports have also implicated $p14^{ARF}$ in p53-independent mechanisms of apoptosis induction.[16,17,33] In the present study, $p14^{ARF}$ restored by DAC treatment might act on the p53-independent mechanisms in the

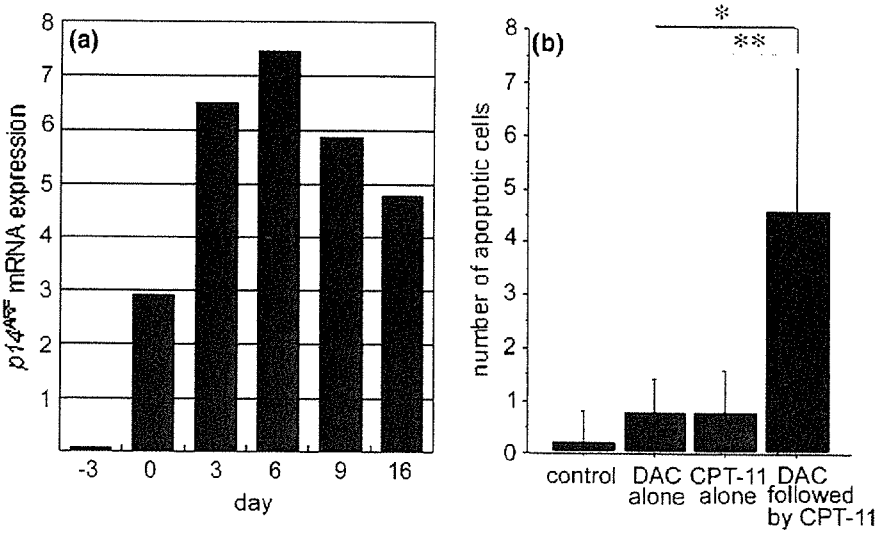

FIG. 4. (a) Real-time polymerase chain reaction (PCR) analysis of *p14ARF* mRNA expression of xenografts. The mice treated with demethylating agent 5-aza-2′-deoxycytidine (DAC) alone (group B in Fig. 3) were killed on days −3, 0, 3, 6, 9, and 16. The tumors were extracted and cDNA synthesized. Relative quantification of *p14ARF* mRNA expression was investigated by real-time PCR. (b) Detection of apoptosis in xenografts by TUNEL (terminal deoxynucleotidyl transferase dUTP nick-end labeling) assay. On day 12 in Fig. 3, the tumor xenografts were extracted from the mice treated with four protocols, then used for TUNEL assay. Data shown are mean number of TUNEL-positive cells counted in 10 fields per slide. $P = .00037$, ** $P = .00042$ (Welch's t-test). Error bars = SD.

TABLE 2. *Analysis of effect of DAC and CTP-11 on tumor xenograft*

Group	Drug	Treatment	TV[a] (mm^3, mean ± SD)	RTV[b] (mean ± SD)	IR[c] (%)	Body weight change[d] (g)	(%, mean ± SD)
A	Control	PBS, day 0, 4, 8	905.0 ± 206.3	9.7 ± 1.0	-	−0.3	1.5 ± 2.0
B	DAC	1 mg/kg × 3, day −3	660.0 ± 106.9	9.2 ± 1.6	5.7	−0.3	1.2 ± 2.2
C	CTP-11	40 mg/kg, day 0, 4, 8	513.6 ± 192.7	7.8 ± 2.4	20.2	−0.2	0.1 ± 0.4
D	DAC + CTP-11		384.8 ± 143.7	2.7 ± 0.6	72.2	+ 0.1	0.3 ± 0.3

[a] Tumor volume (TV) on day 16 = (width) × (width) × (length)/2.
[b] Relative Tumor volume (RTV) = (TV on day 16)/(TV on day 0).
[c] Inhibition rate on tumor growth (IR) = {1 − (mean RTV of the treatment group)/(mean RTV of the control group)} × 100.
[d] Body weight change (BWC) = (BW on day 16)−(BW on day−3). BWC(%) = (BWC on day 16)/(BWC on day −3) × 100.

apoptotic pathway because HCT-15 cells lack normal p53 expression because of a point mutation. Overexpression of *BNIP3*, which is a proapoptotic gene, increased the sensitivity to apoptosis induced by topoisomerase I and II.[34] In some kinds of cancers, *BNIP3* was reported to be inactivated by aberrant hypermethylation.[35,36] *XAF1* is a 34-kDa zinc finger protein that blocks the caspase-inhibiting and antiapoptotic abilities of X-linked inhibitor of apoptosis protein. The association between the reduction of *XAF1* expression and its aberrant hypermethylation has been reported.[37–39] Restoration of *XAF1* expression by DAC might be one of the potential mechanisms involved in the effect of DAC on CPT-11 sensitivity. Moreover, DAC might enhance another pro-apoptotic pathway through demethylation of other genes. Indeed, we confirmed aberrant hypermethylation of other pro-apoptotic genes (i.e., *DAPK*, *Apaf-1* and *TMS1*: data not shown). Taken together, our study suggests that DAC might exert an effect on the sensitivity of cancer cells to CPT-11 by restoring the silenced gene expression because of aberrant hypermethylation participating in the inactivation of the apoptotic pathway at several points.

In this study, DAC decreased *bcl-2* mRNA expression in a dose-dependent manner. Violette et al.[40] reported that the balance of bax, bcl-2, and bcl-X_L (bcl-2 + bcl-X_L/bax) could be used as a marker to predict the pro-apoptotic ability and chemosensitivity, regardless of the p53 status. In this study, DAC did not influence *bax* expression, but decreased *bcl-2* expression in HCT-15, although the mechanisms

involved are unknown. Therefore, DAC might shift this balance to the pro-apoptotic side and might enhance the pro-apoptotic ability in HCT-15 cells.

Tan et al.[41] and Rasheed and Rubin[42] reported that the expression and activity of topo-I, the target enzyme of CPT-11, correlated to the chemosensitivity of CPT-11. In contrast, Bras-Goncalves et al.[43] reported that the expression level of *topo-I* mRNA did not correlate with the CPT-11 response of the tumor. In this study, DAC did not influence the expression level of *topo-I* mRNA but increased the effect of CPT-11 on growth inhibition, suggesting that the expression level of *topo-I* mRNA is unlikely to be associated with HCT-15 response to CPT-11, which is consistent with the report by Bras-Goncalves et al.

We thought that the most suitable dose of DAC was the minimum dose in which silenced gene expression was restored and cell proliferation was not affected. According to a previous report,[23] induction of gene expression by DAC was observed in .1 to 1 μM of DAC in plasma level. In our study in vitro, we confirmed that demethylation and gene reexpression were also observed in .1 μM of DAC (Fig. 1). In our preliminary experiments of growth inhibition in vitro, cell proliferation was interfered with in 1 μM of DAC but not in .1 and .5 μM of DAC compared with untreated control (data not shown). In the combined therapy with DAC and SN-38, the growth inhibition was more apparent in .5 μM of DAC compared with .1 μM of DAC (data not shown). So we determined .5 μM to be the most suitable dose of DAC for in vitro studies.

In experiments in vivo with ovarian cancer cells xenograft, Plumb et al.[19] described that the most effective and nontoxic regimen was three doses of 5 mg·kg of DAC at intervals of 3 hours (total dose, 15 mg·kg). However, our preliminary experiments showed that three doses of 5 mg·kg of DAC produced adverse effects such as weight loss and severe diarrhea when combined with CPT-11 (data not shown). We also confirmed that the tumor growth was reduced when mice were treated with DAC followed by CPT-11, but there was no difference in the tumor growth between three doses of 1 and 3 mg·kg (data not shown). From these observations, we determined three doses of 1 mg·kg of DAC at intervals of 3 hours to be the best dose of DAC for in vivo studies. This dose was the minimum that did not inhibit tumor growth, but it restored and maintained the $p14^{ARF}$ mRNA expression, and the combined therapy of DAC followed by CPT-11 in vivo could produce synergistic growth inhibition without causing major toxicity, as in the in vitro study.

One of the most important findings in this study was the duration of the demethylation status after DAC treatment. Through our in vitro study, expression of $p14^{ARF}$ mRNA in HCT-15 cells was at its maximum 9 days after DAC was added and was sustained for longer than 30 days after DAC's removal on day 3. This result may support the idea that epigenetic change can be inherited in DNA replication, implying that the demethylation status in the tumor would continue after DAC has disappeared from the plasma in vivo. Therefore, when DAC is used as a "biosensitizer," it might as well be administered before anticancer drugs.

DAC has already been used in clinical trials on hematopoietic malignancies, and a 20% to 30% response rate has been demonstrated.[13,14,44,45] However, preliminary experiences with demethylating agents in solid tumors have been disappointing because the response rates have been low.[13,21,46,47] Most clinical studies of DAC in solid tumors have also failed to inhibit tumor progression, and response rates have generally failed to exceed 10%.[13] However, these discouraging results were in trials that used DAC alone. Therefore, to induce apoptosis after DAC treatment, some DNA damage may be required as a trigger. We hypothesized that almost all chemotherapeutic drugs and irradiation could act as a trigger and might show some synergistic effect when combined with DAC.

In solid tumors, the clinical usefulness of combined therapy with DAC and CPT-11 has not been fully investigated. Plumb et al.[19] reported that DAC treatment enhanced the sensitivity of CRC xenografts to anticancer drugs including cisplatin, epirubicin, and carboplatin. Anzai et al.[48] reported on the synergistic effect of DAC and topotecan in murine CRC cells, but they did not sufficiently investigate the mechanism of synergy. Pohlmann et al.[49] performed a phase 2 trial of cisplatin plus DAC in patients with advanced squamous cell carcinoma of the cervix and demonstrated that this combination therapy was moderately effective. However, the regimen used in that trial produced hematologic toxicities. Previous clinical studies have seemed to adhere to maintaining a plasma concentration of DAC, which led to severe toxicity. When we recognized reexpression gene products as a target for BRMs, DAC could be used at lower doses associated with a biological effect on the target tissues. We think that the most important finding regarding DAC treatment is to sustain the gene expression in the tumor, but not to maintain a high plasma concentration of DAC. Therefore, we propose that DAC can be effectively provided at a